

Electronic Supplementary Information

Homochiral layered indium phosphonates: solvent modulation of morphology and chiral discrimination adsorption

Qian Teng, Song-Song Bao, Ran Gao, Li-Min Zheng*

State Key Laboratory of Coordination Chemistry, School of Chemistry and Chemical Engineering, Collaborative Innovation Center of Advanced Microstructures, Nanjing University, Nanjing 210023, P. R. China

* Corresponding author. E-mail: lmzheng@nju.edu.cn

Table S1 Crystal data and structure refinements for **S-1C**.

Compounds	S-1C
Formula	C ₁₈ H ₃₂ In ₂ N ₄ O ₁₆ P ₂
<i>M</i>	852.05
Crystal system	monoclinic
Space group	<i>P</i> 2 ₁
<i>a</i> (Å)	18.9319(9)
<i>b</i> (Å)	7.7064(4)
<i>c</i> (Å)	10.0756(5)
β (°)	102.547(2)
<i>V</i> (Å ³)	1434.89(12)
<i>Z</i>	2
<i>D_c</i> (g cm ⁻³)	1.972
<i>μ</i> (mm ⁻¹)	9.926
<i>F</i> (000)	848.0
<i>R_{int}</i>	0.0566
GoF on <i>F</i> ²	1.108
<i>R</i> ₁ , <i>wR</i> ₂ ^[a] [<i>I</i> > 2σ(<i>I</i>)]	0.0407, 0.1189
CCDC	2402002

$$R_1 = \sum ||F_o| - |F_c|| / \sum |F_o|, wR_2 = [\sum w(F_o^2 - F_c^2)^2 / \sum w(F_o^2)^2]^{1/2}$$

TableS2. Selected bond lengths [\AA] and bond angles [$^\circ$] of **S-1C**.

In1-O1	2.132(7)	In2-O2	2.137(7)	P1-O1	1.499(7)
In1-O3A	2.137(6)	In2-O5	2.118(7)	P1-O2	1.524(7)
In1-O4	2.124(7)	In2-O6B	2.136(7)	P1-O3	1.531(7)
In1-O7	2.081(7)	In2-O8	2.097(7)	P2-O4	1.521(7)
In1-O7A	2.092(7)	In2-O8C	2.090(7)	P2-O5	1.502(7)
In1-O1W	2.227(7)	In2-O2W	2.223(7)	P2-O6	1.517(7)
O1-In1-O3A	170.9(3)	O7-In1-O4	93.7(3)	O8-In2-O2	94.8(3)
O1-In1-O1W	87.3(3)	O7-In1-O7A	172.14(12)	O8C-In2-O5	92.4(3)
O3A-In1-O1W	83.7(3)	O7-In1-O1W	86.5(3)	O8-In2-O5	84.0(3)
O4-In1-O1	97.1(3)	O7A-In1-O1W	86.8(3)	O8C-In2-O6B	88.5(2)
O4-In1-O3A	91.9(3)	O2-In2-O2W	177.7(3)	O8-In2-O6B	93.9(3)
O4-In1-O1W	175.6(3)	O5-In2-O2	95.7(3)	O8C-In2-O8	172.06(12)
O7-In1-O1	91.2(3)	O5-In2-O6B	170.8(4)	O8-In2-O2W	86.5(3)
O7A-In1-O1	84.4(3)	O5-In2-O2W	86.3(3)	O8C-In2-O2W	86.2(3)
O7A-In1-O3A	95.2(3)	O6B-In2-O2	93.4(3)	In1-O7-In1D	135.6(3)
O7-In1-O3A	88.2(2)	O6B-In2-O2W	84.7(3)	In2B-O8-In2	134.7(3)
O7A-In1-O4	93.3(3)	O8C-In2-O2	92.6(3)		

Symmetry transformations used to generate equivalent atoms: A: -x+1, y-1/2, -z+1; B:-x+1, y+1/2, -z; C: -x+1, y-1/2, -z; D: -x+1, y+1/2, -z+1.

TableS3. Hydrogen bonds in **S-1C**.

D-H···A	d(D-H) [\AA]	d(H···A) [\AA]	d(D···A) [\AA]	<DHA [$^\circ$]
O7-H7···O14	0.85	2.15	2.952(12)	158
O8-H8···O11	0.85	2.44	3.253(13)	160
O1W-H1WA···O12	0.90	2.04	2.922(13)	167
O1W-H1WB···O6	0.90	1.89	2.779(10)	167
O2W-H2WA···O9	0.90	2.04	2.916(12)	165
O2W-H2WB···O3	0.90	1.93	2.791(10)	159
N1-H1A···O14	0.91	2.03	2.889(19)	157
N1-H1B···O10	0.91	1.95	2.852(11)	174
N2-H2A···O11	0.91	2.09	2.976(19)	163
N2-H2B···O13	0.91	1.96	2.872(11)	179

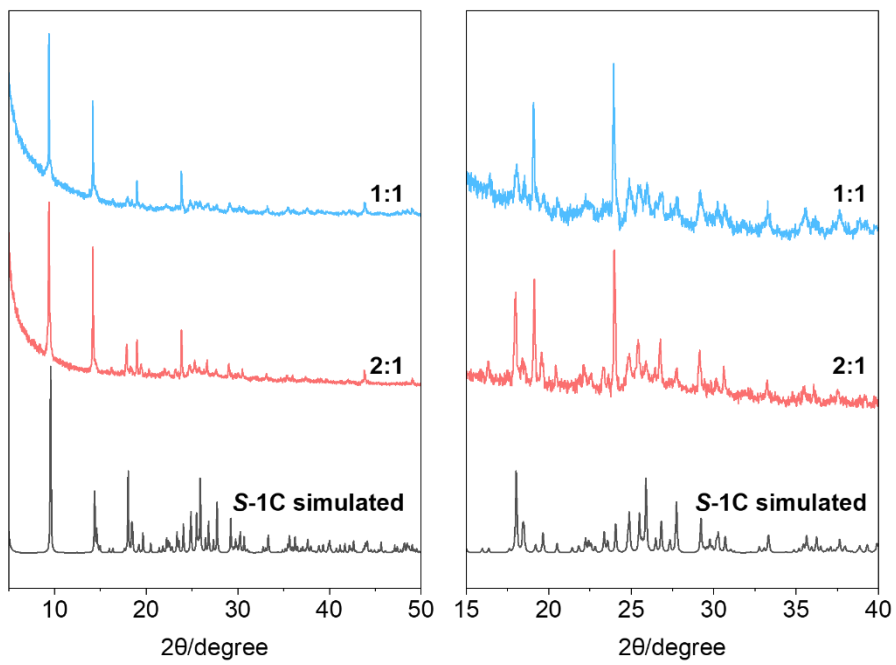


Fig. S1. PXRD patterns of the reaction products after solvothermal reactions of $\text{In}(\text{NO}_3)_3 \cdot 5\text{H}_2\text{O}$ and S-pempH₂ in 50 vol% TEG/H₂O at 100°C, when metal:ligand molar ratio were 2:1 and 1:1.

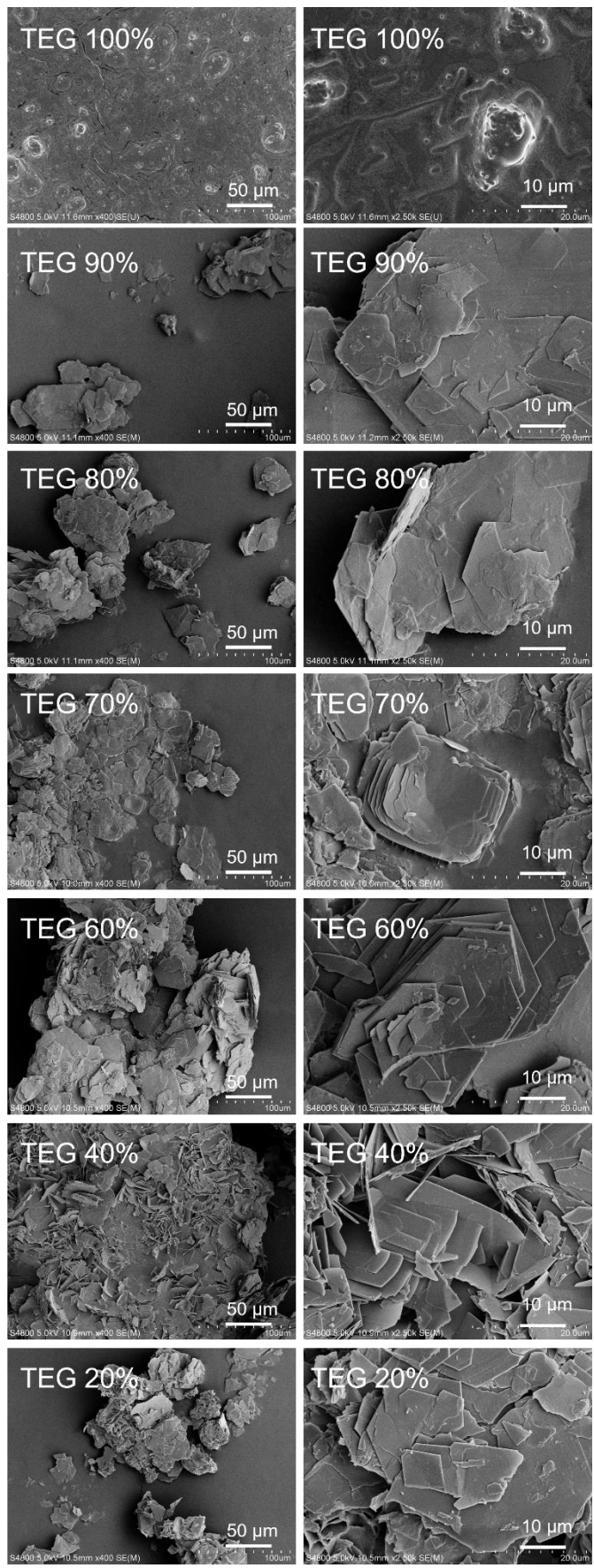


Fig. S2. SEM images showing the morphology of reaction products of $\text{In}^{3+}/\text{S-pempH}_2$ (2:1) obtained in different volume ratio of TEG/H₂O (total volume 10 mL) at 100 °C.

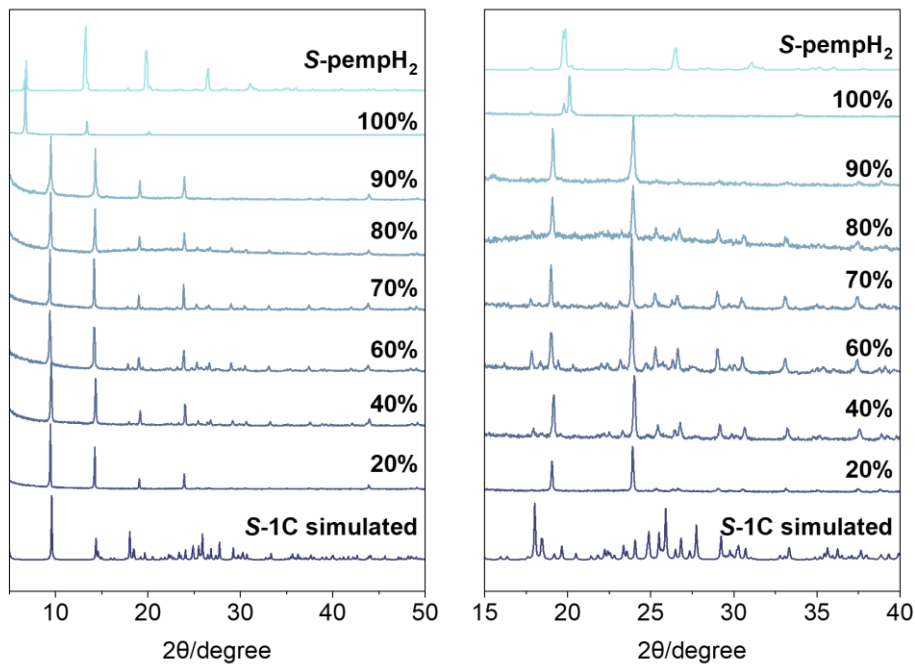


Fig. S3. PXRD patterns of the reaction products of $\text{In}^{3+}/\text{S-pempH}_2$ (2:1) obtained in different volume ratio of TEG/H₂O (total volume 10 mL) at 100 °C.

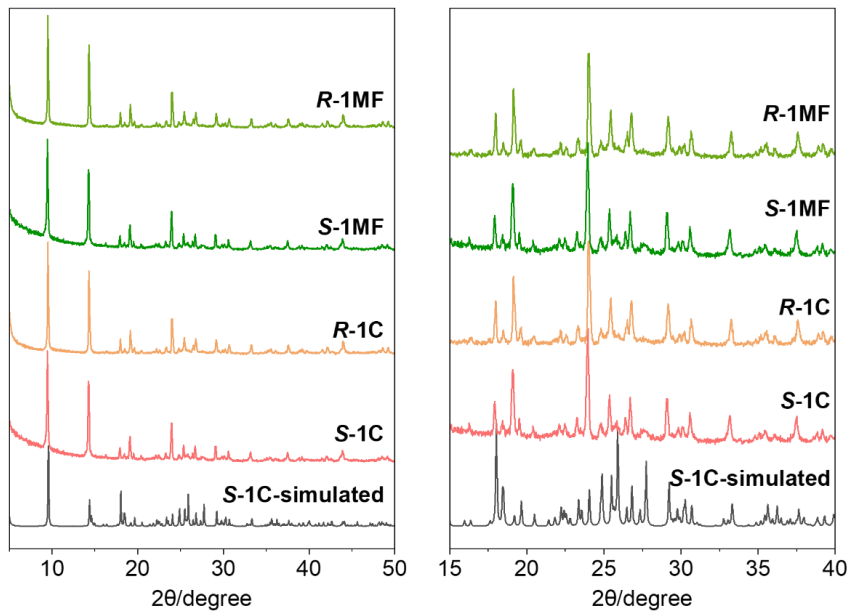


Fig. S4. PXRD patterns of simulated from the single-crystal data of **S-1C**, as-synthesized **R-**, **S-1C** and **R-**, **S-1MF**.

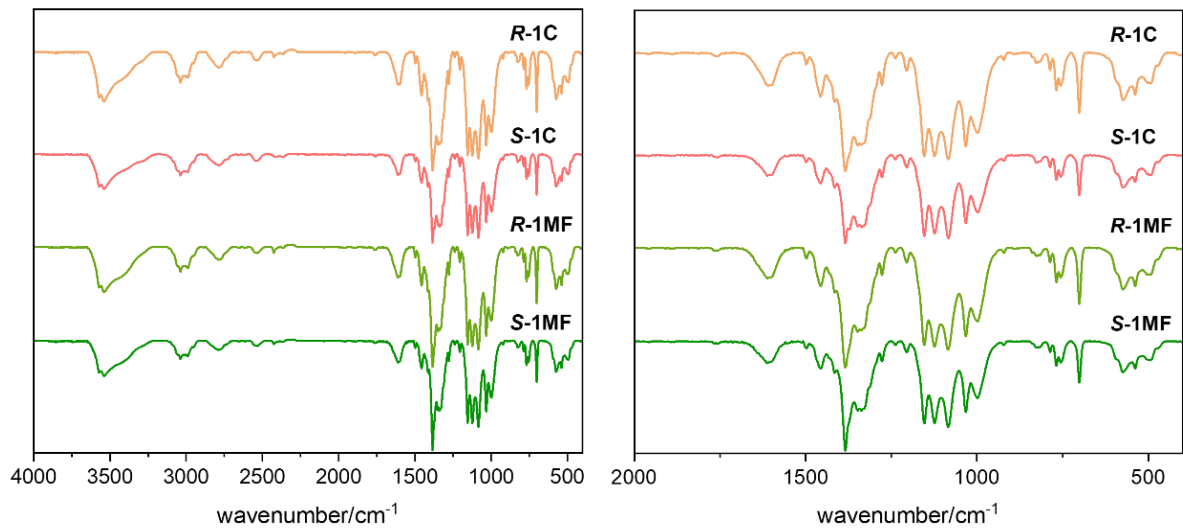


Fig. S5. The IR spectra of **R**, **S-1C** and **R**, **S-1MF** (Left: 4000–400 cm^{-1} , Right: 2000–400 cm^{-1}).

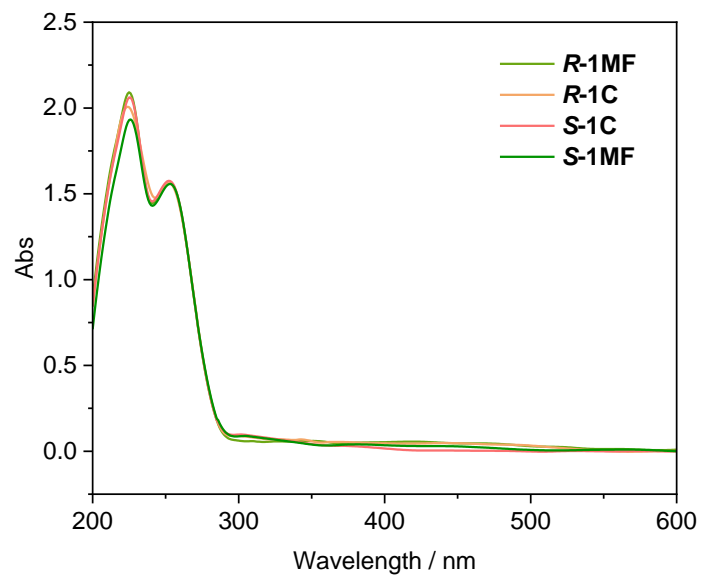


Fig. S6. The UV-Vis absorption spectra of **R**, **S-1C** and **R**, **S-1MF**.

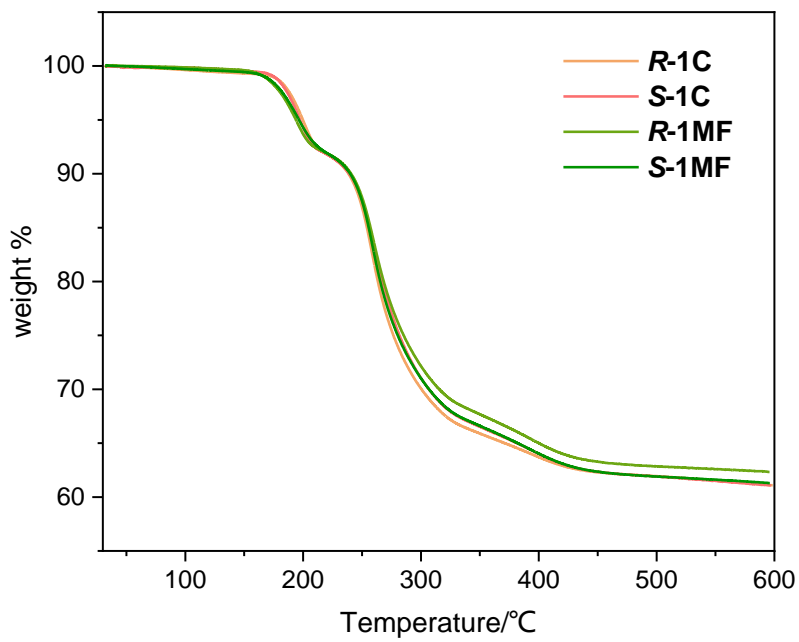


Fig. S7. TGA curves of **R-**, **S-1C** and **R-**, **S-1MF**.

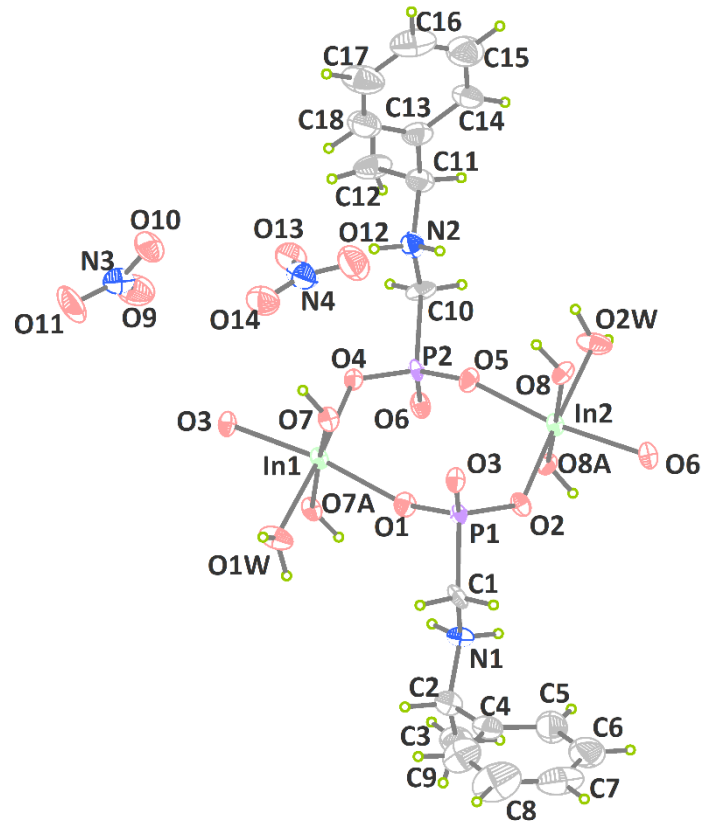


Fig. S8. Coordination environment of the asymmetric unit in **S-1C**.

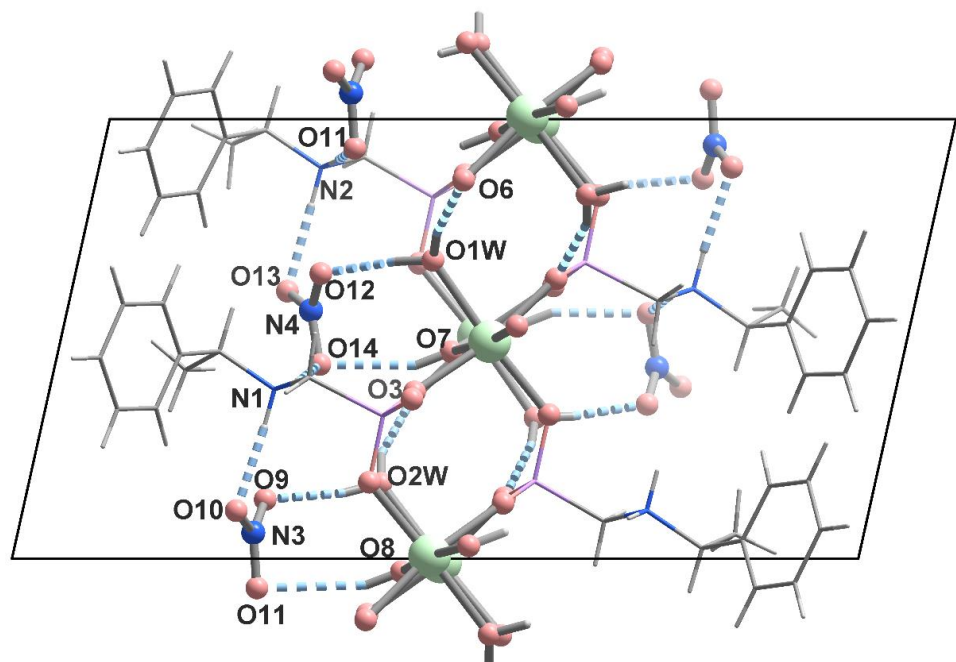


Fig. S9. Packing diagrams of structures of **S-1C**. The dotted lines represent the hydrogen bonding interactions.

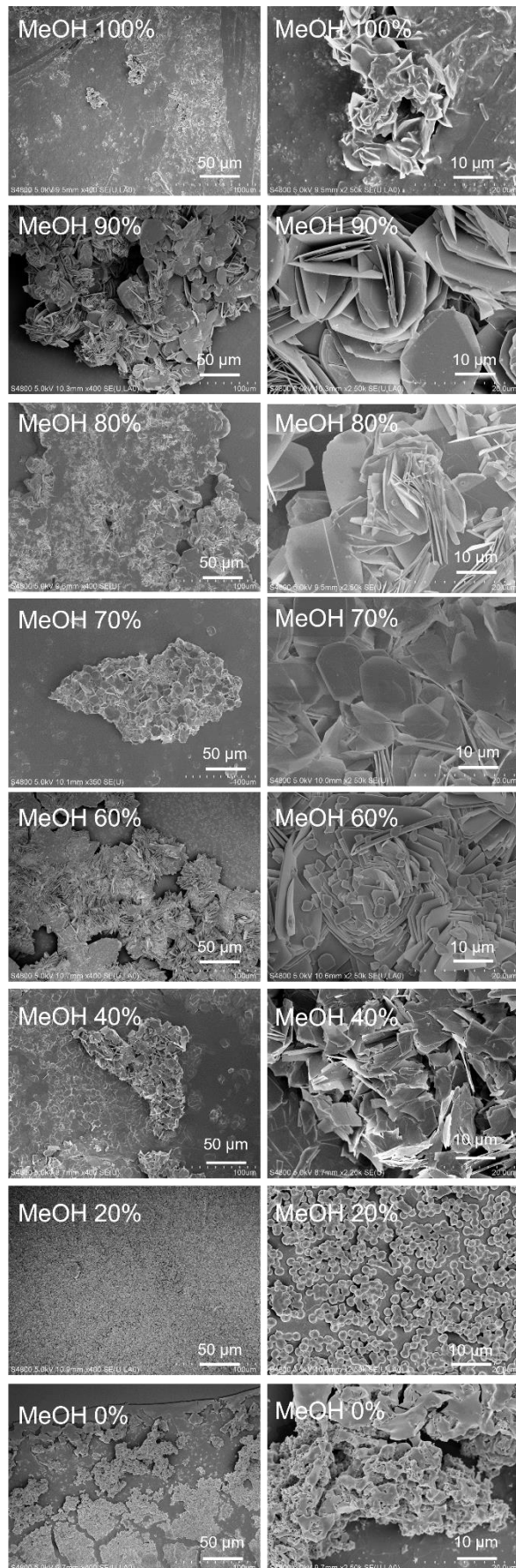


Fig. S10. SEM images showing the morphology of reaction products of $\text{In}(\text{NO}_3)_3/\text{S-pempH}_2$ (1:1) obtained in different volume ratio of $\text{MeOH}/\text{H}_2\text{O}$ (total volume 10 mL) at 100 °C.

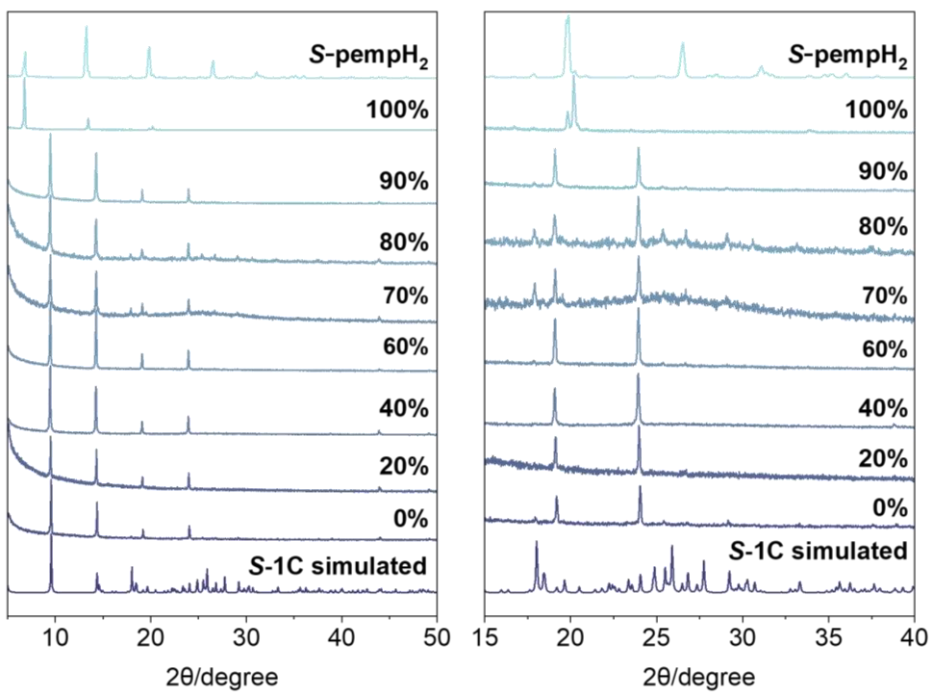


Fig. S11. PXRD patterns of the reaction products of $\text{In}(\text{NO}_3)_3$ /S-pempH₂ (1:1) obtained in different volume ratio of MeOH/H₂O (total volume 10 mL) at 100 °C.

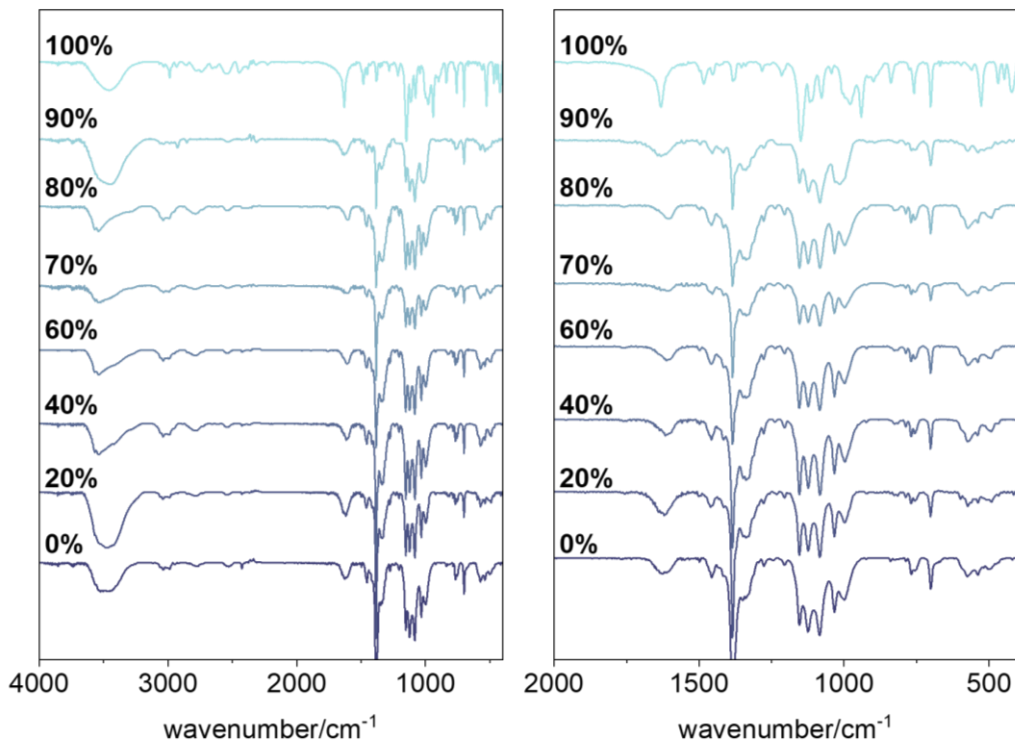


Fig. S12 IR spectra of the reaction products of $\text{In}(\text{NO}_3)_3$ /S-pempH₂ (1:1) obtained in different volume ratio of MeOH/H₂O (total volume 10 mL) at 100 °C.

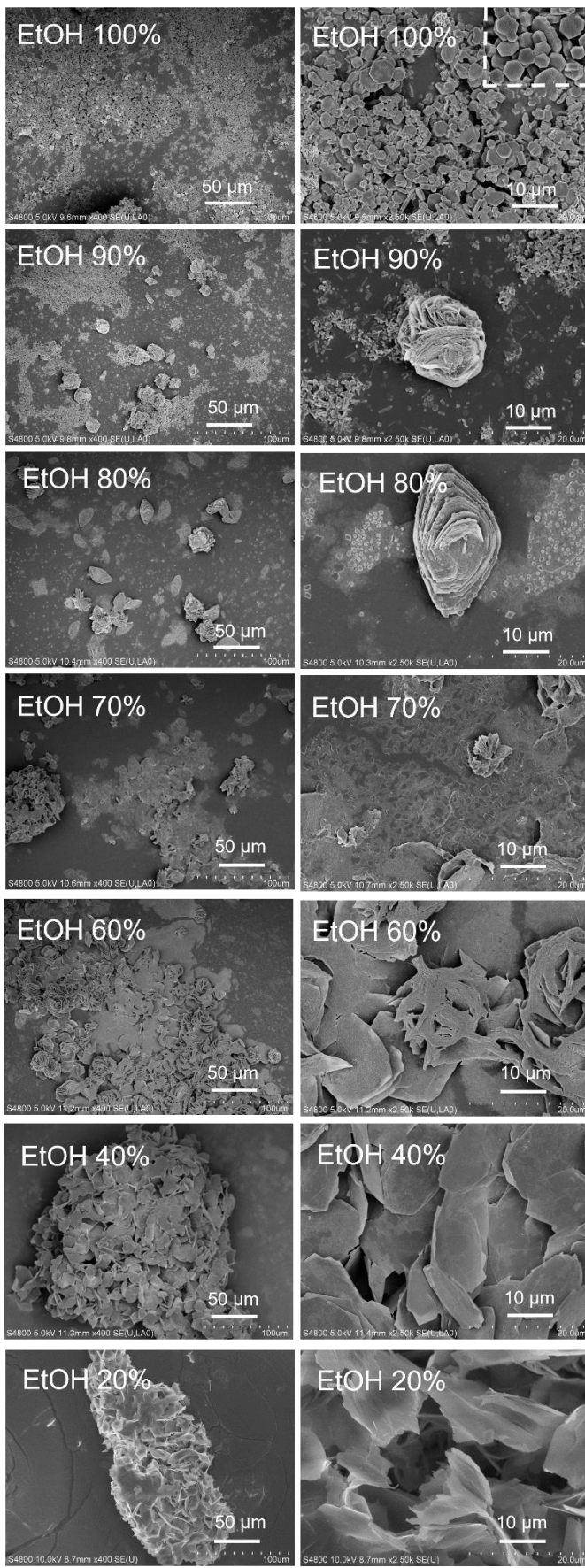


Fig. S13. SEM images showing the morphology of reaction products of $\text{In}(\text{NO}_3)_3/\text{S-pempH}_2$ (1:1) obtained in different volume ratio of EtOH/ H_2O (total volume 10 mL) at 100 °C.

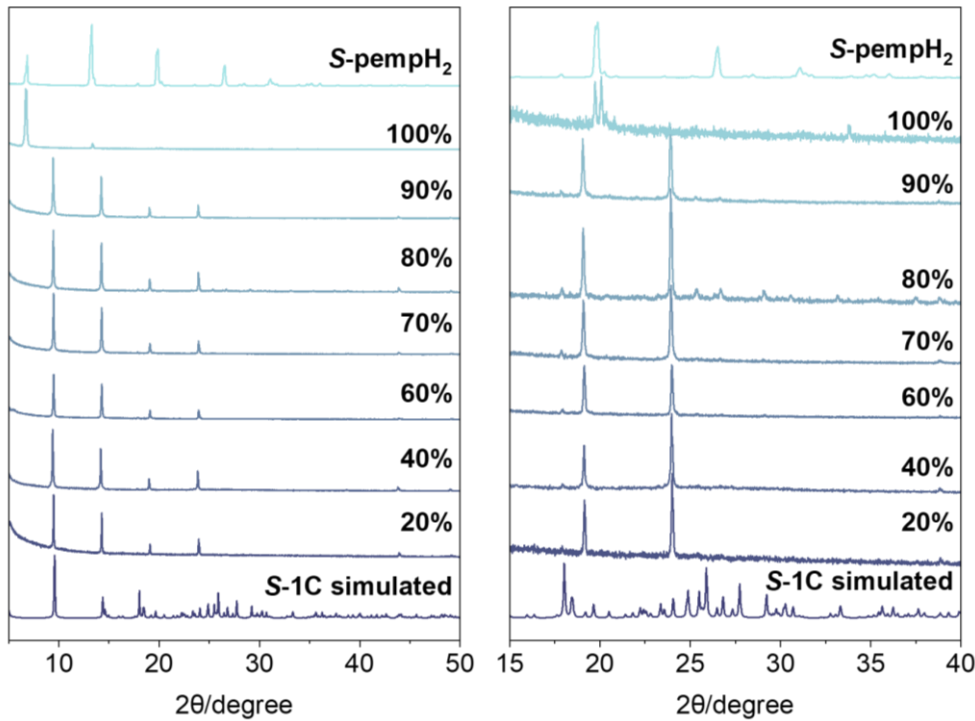


Fig. S14. PXRD patterns of the reaction products of $\text{In}(\text{NO}_3)_3/\text{S-pempH}_2$ (1:1) obtained in different volume ratio of $\text{EtOH}/\text{H}_2\text{O}$ (total volume 10 mL) at 100 °C.

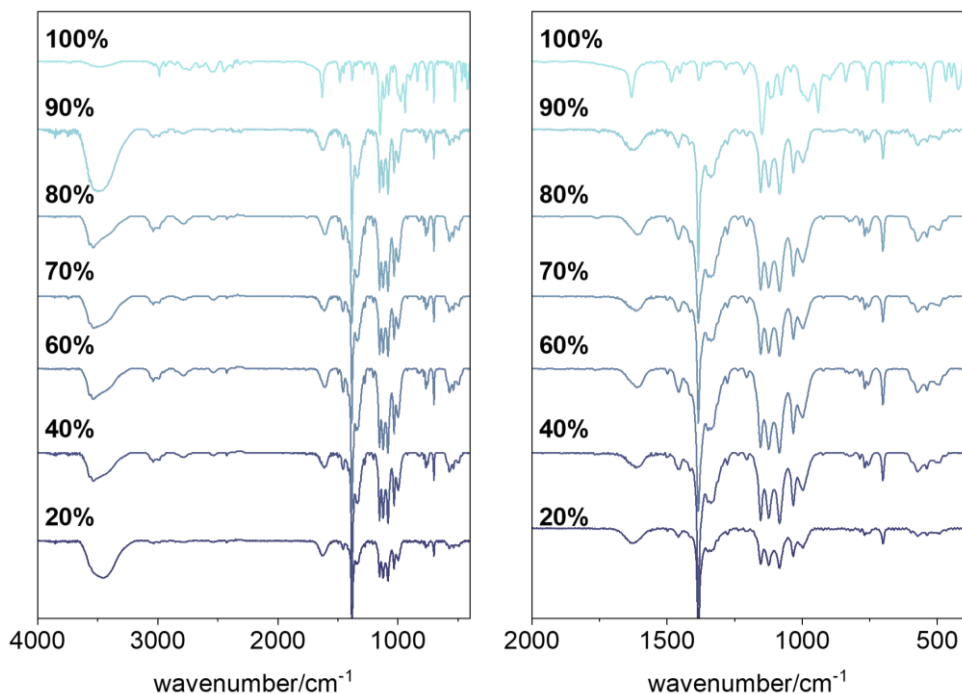


Fig. S15. IR spectra of the reaction products of $\text{In}(\text{NO}_3)_3/\text{S-pempH}_2$ (1:1) obtained in different volume ratio of $\text{EtOH}/\text{H}_2\text{O}$ (total volume 10 mL) at 100 °C.

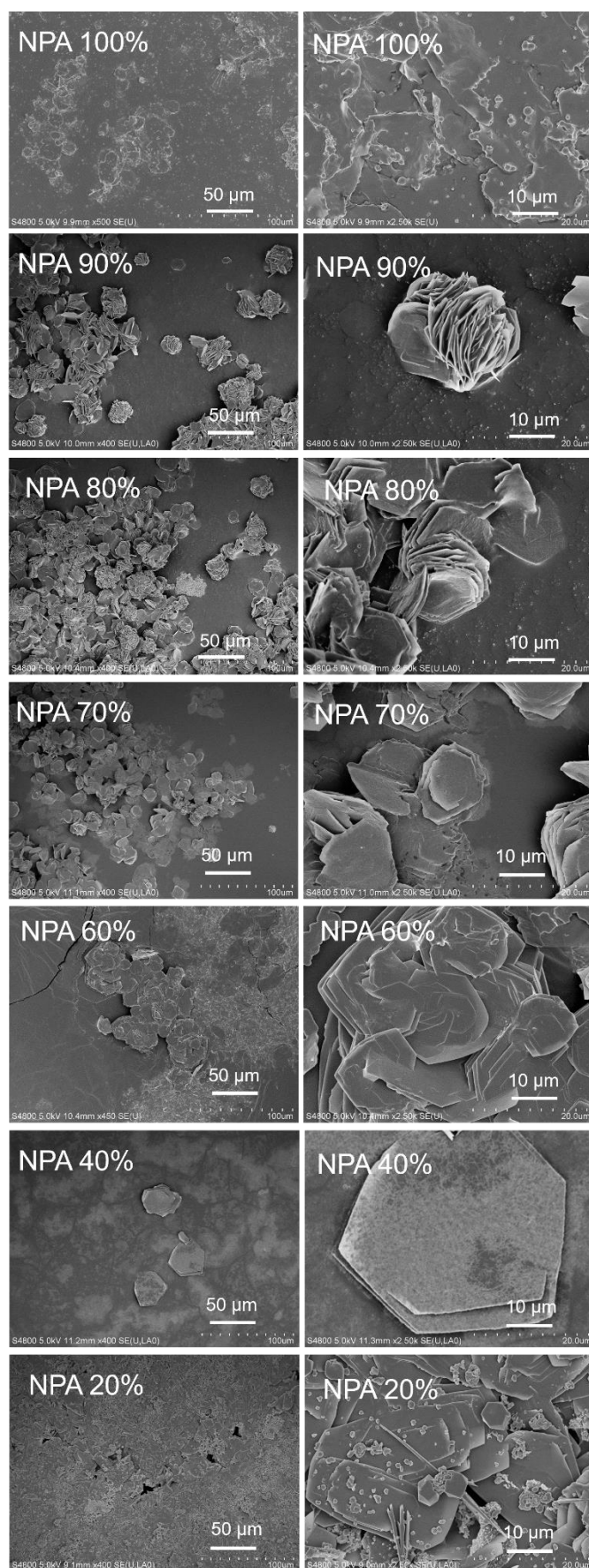


Fig. S16. SEM images showing the morphology of reaction products of $\text{In}(\text{NO}_3)_3/\text{S-pempH}_2$ (1:1) obtained in different volume ratio of NPA/ H_2O (total volume 10 mL) at 100 °C.

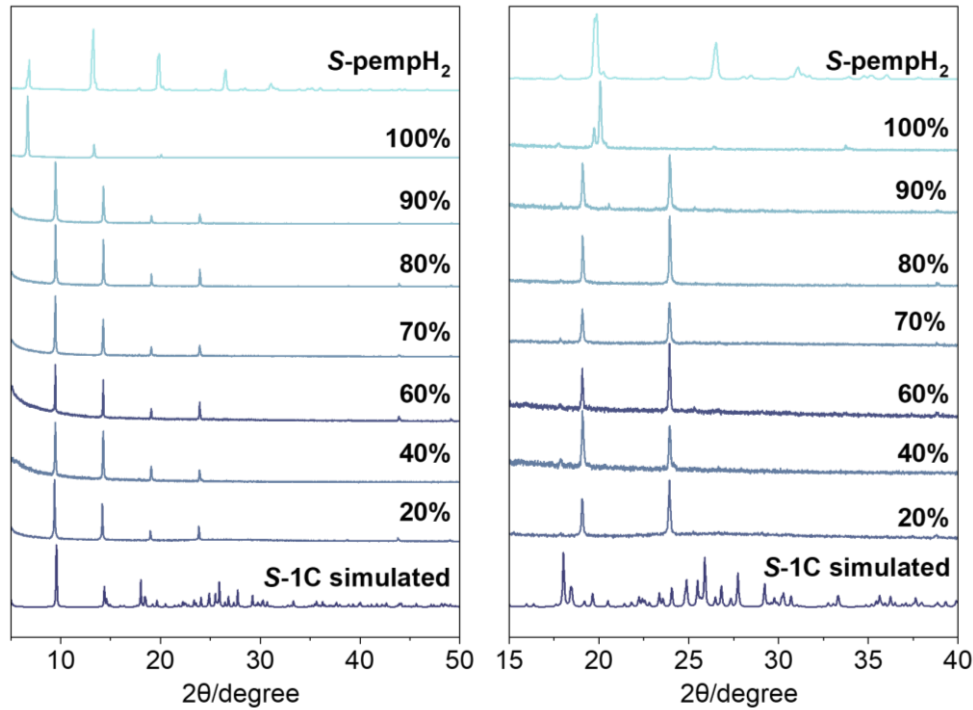


Fig. S17. PXRD patterns of the reaction products of $\text{In}(\text{NO}_3)_3/\text{S-pempH}_2$ (1:1) obtained in different volume ratio of NPA/ H_2O (total volume 10 mL) at 100 °C.

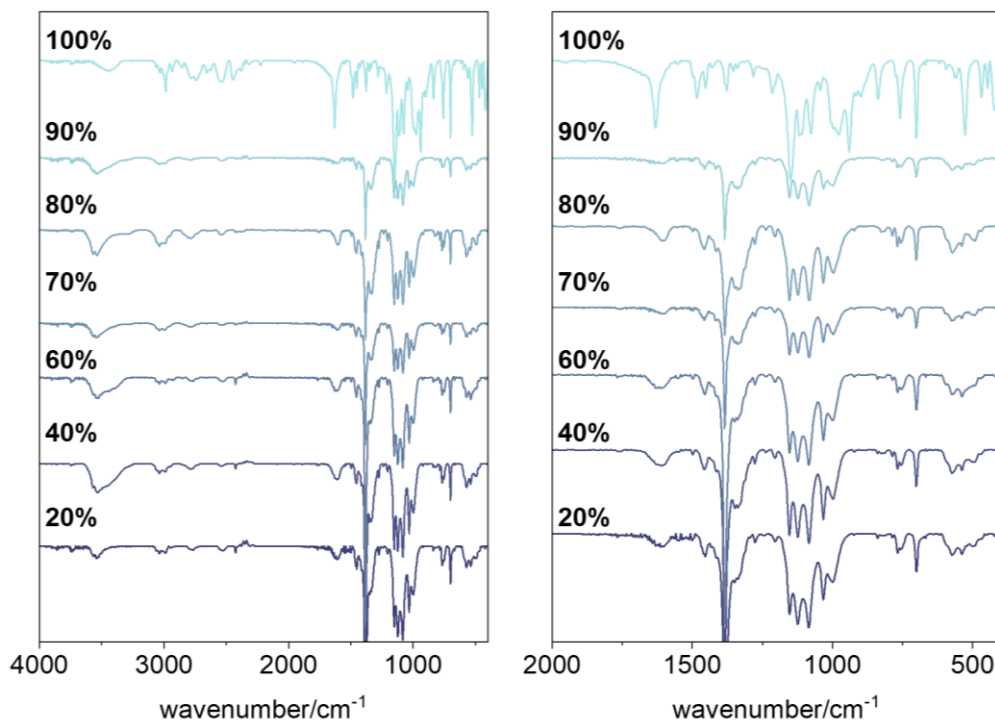


Fig. S18. IR spectra of the reaction products of $\text{In}(\text{NO}_3)_3/\text{S-pempH}_2$ (1:1) obtained in different volume ratio of NPA/ H_2O (total volume 10 mL) at 100 °C.

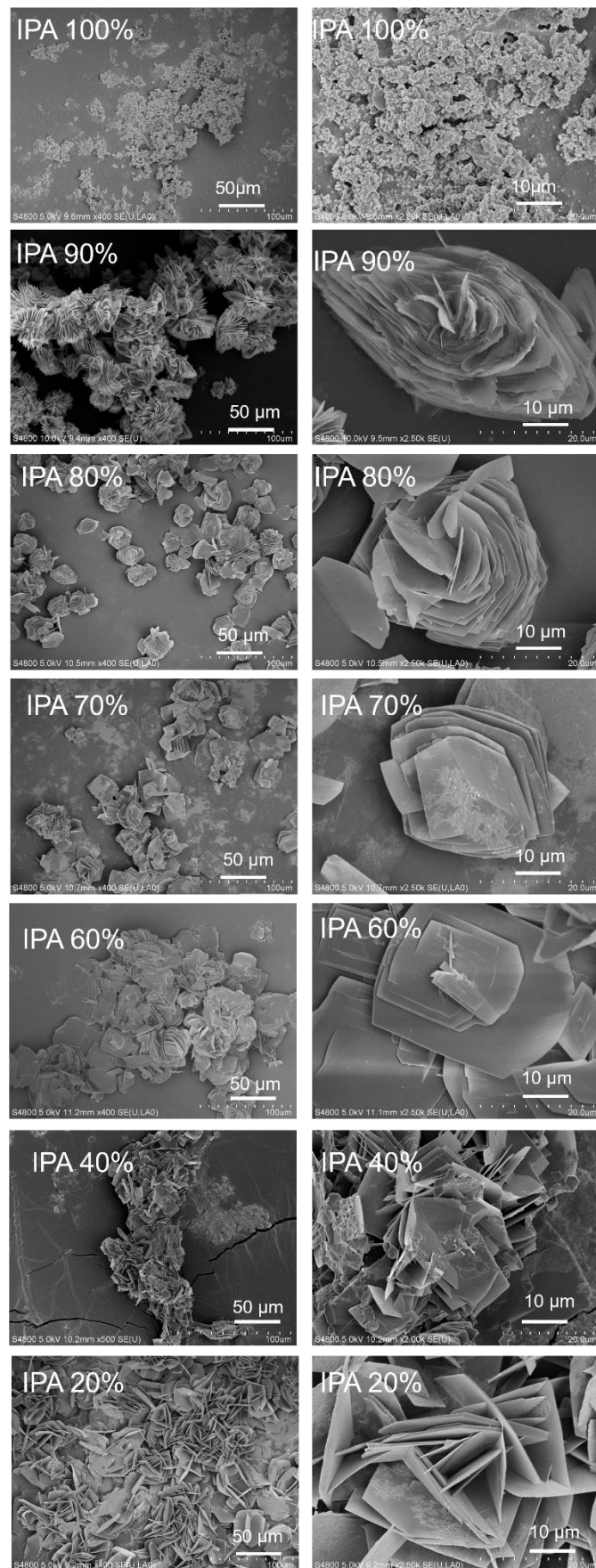


Fig. S19. SEM images showing the morphology of reaction products of $\text{In}(\text{NO}_3)_3/\text{S-pempH}_2$ (1:1) obtained in different volume ratio of IPA/ H_2O (total volume 10 mL) at 100 °C.

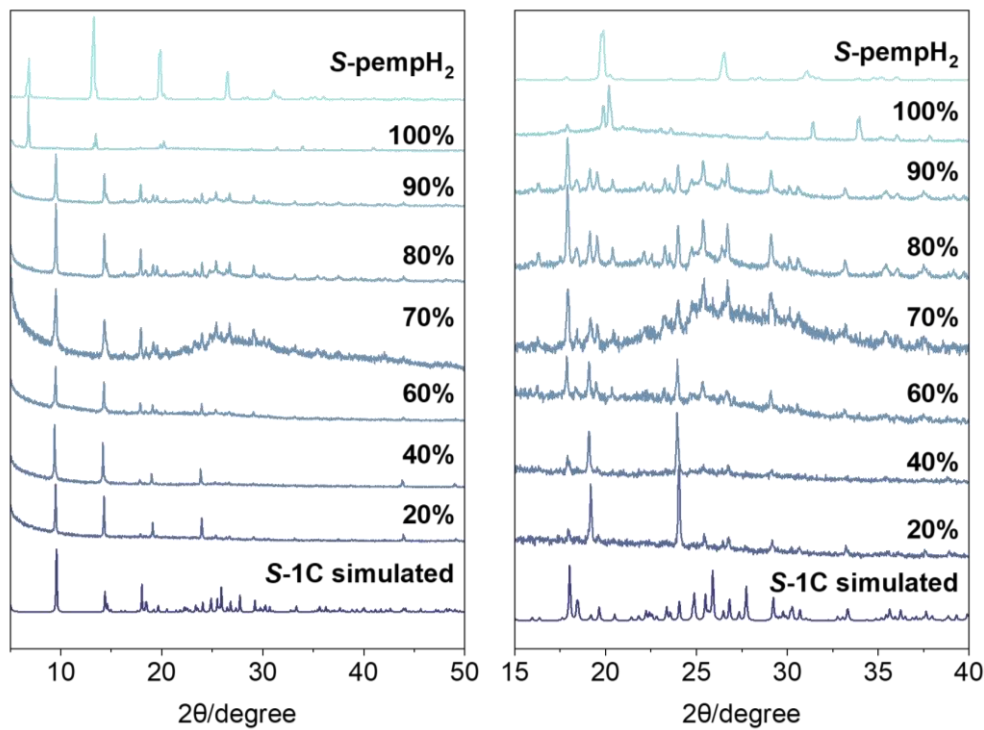


Fig. S20. PXRD patterns of the reaction products of $\text{In}(\text{NO}_3)_3$ /S-pempH₂ (1:1) obtained in different volume ratio of IPA/H₂O (total volume 10 mL) at 100 °C.

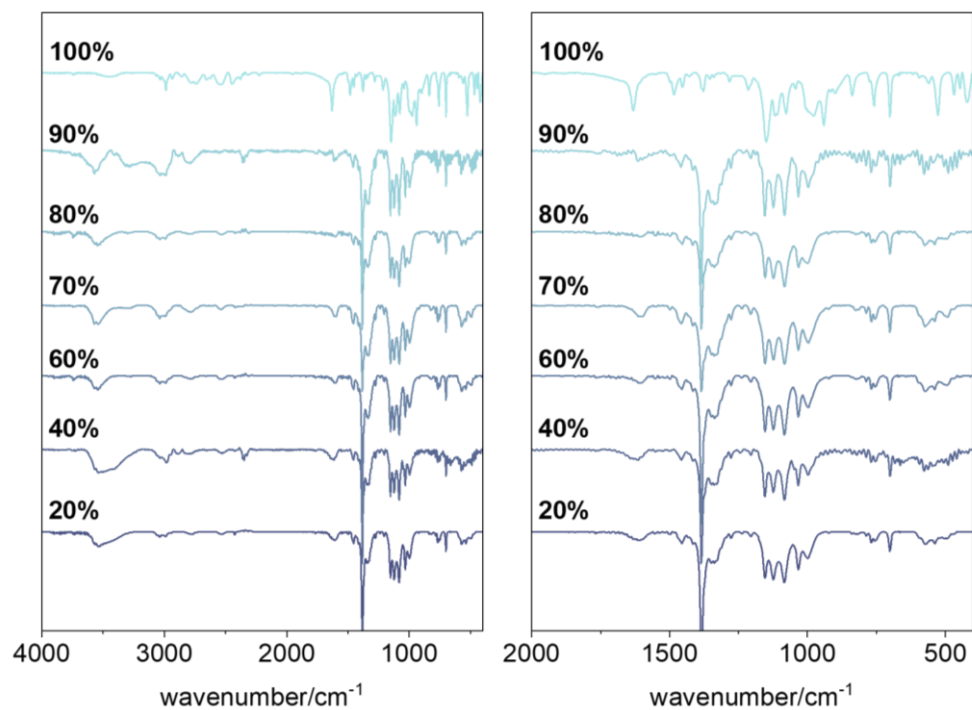


Fig. S21. IR spectra of the reaction products of $\text{In}(\text{NO}_3)_3$ /S-pempH₂ (1:1) obtained in different volume ratio of IPA/H₂O (total volume 10 mL) at 100 °C.

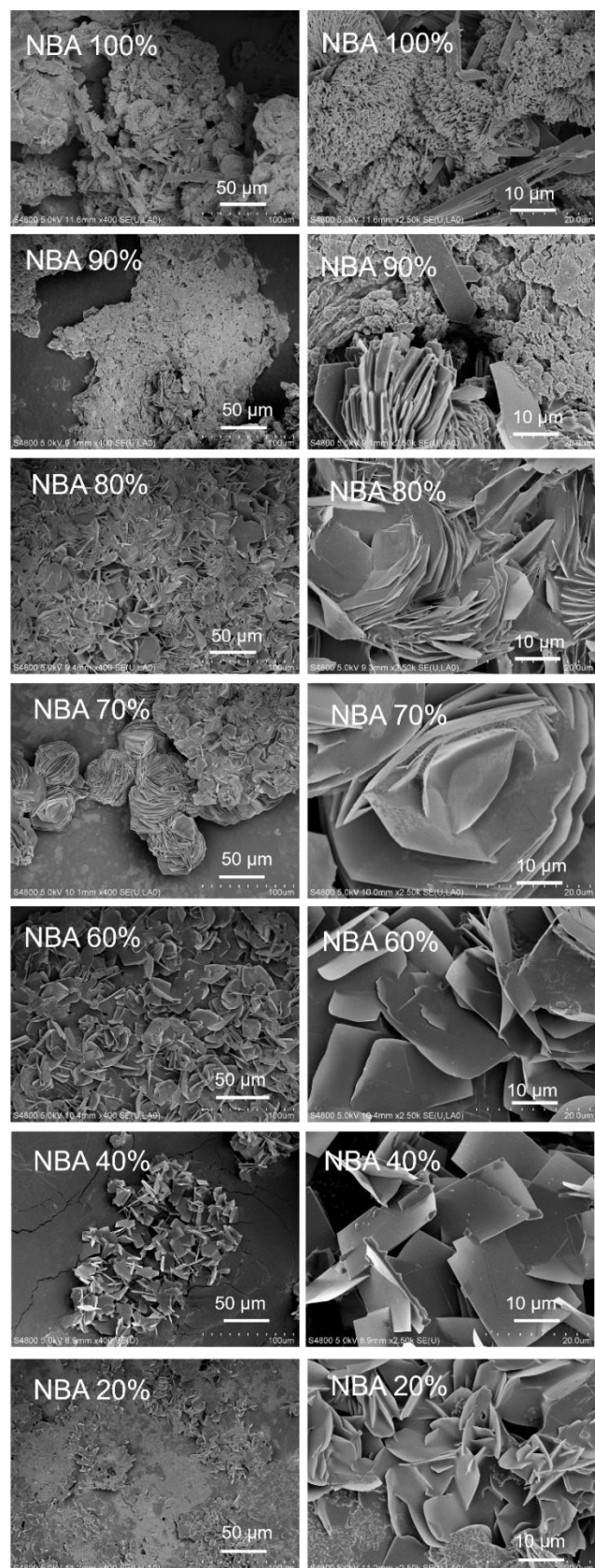


Fig. S22. SEM images showing the morphology of reaction products of $\text{In}(\text{NO}_3)_3/\text{S}\text{-pempH}_2$ (1:1) obtained in different volume ratio of NBA/H₂O (total volume 10 mL) at 100 °C.

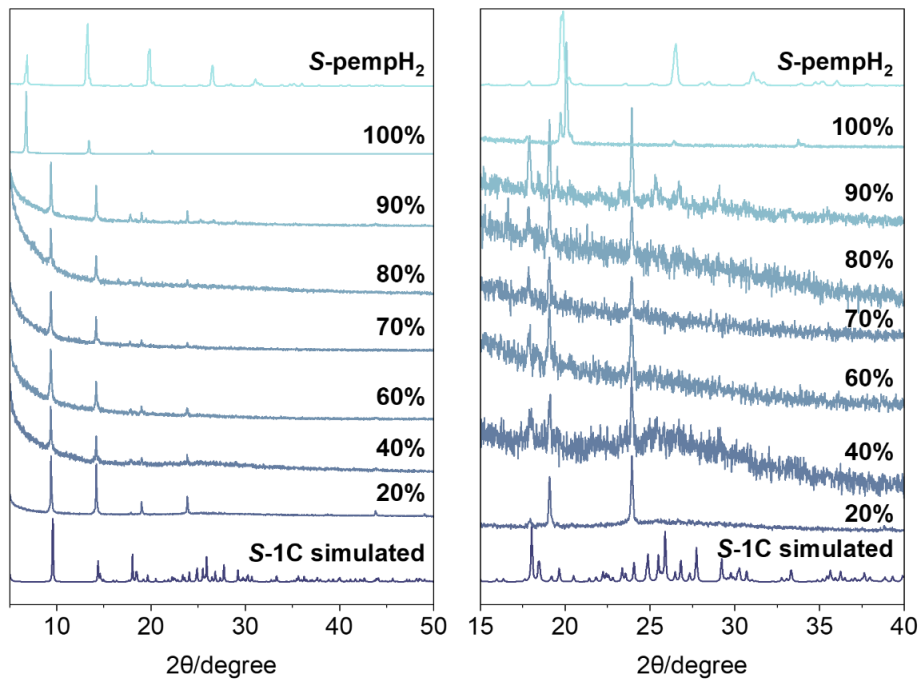


Fig. S23. PXRD patterns of the reaction products of $\text{In}(\text{NO}_3)_3/\text{S-pempH}_2$ (1:1) obtained in different volume ratio of $\text{NBA}/\text{H}_2\text{O}$ (total volume 10 mL) at 100 °C.

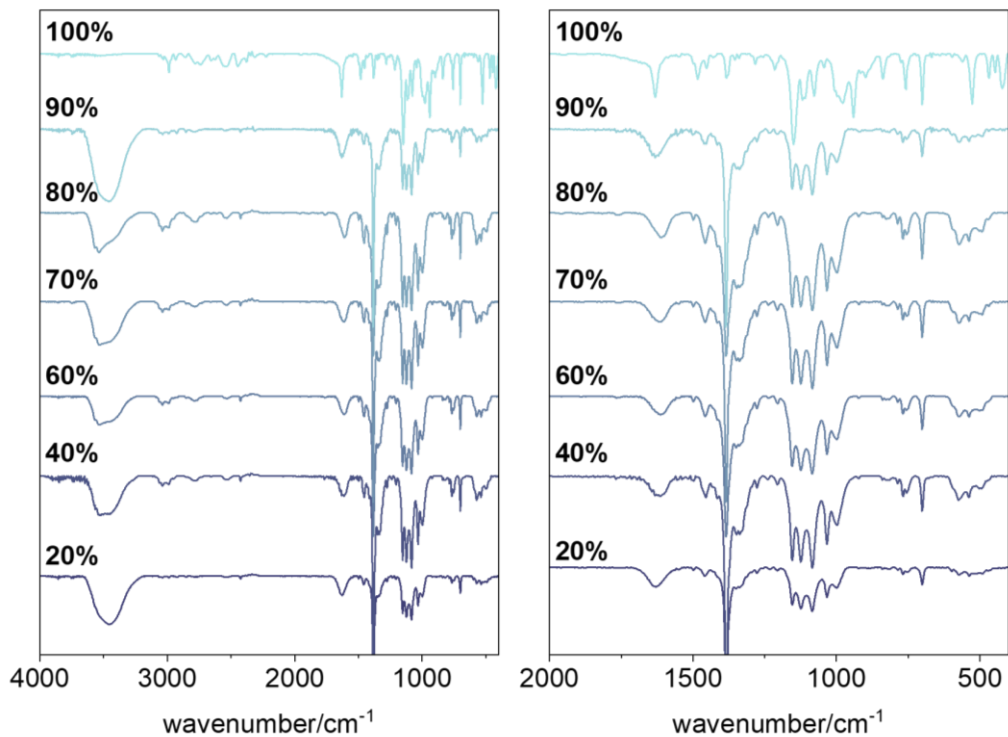


Fig. S24. IR spectra of the reaction products of $\text{In}(\text{NO}_3)_3/\text{S-pempH}_2$ (1:1) obtained in different volume ratio of $\text{NBA}/\text{H}_2\text{O}$ (total volume 10 mL) at 100 °C.

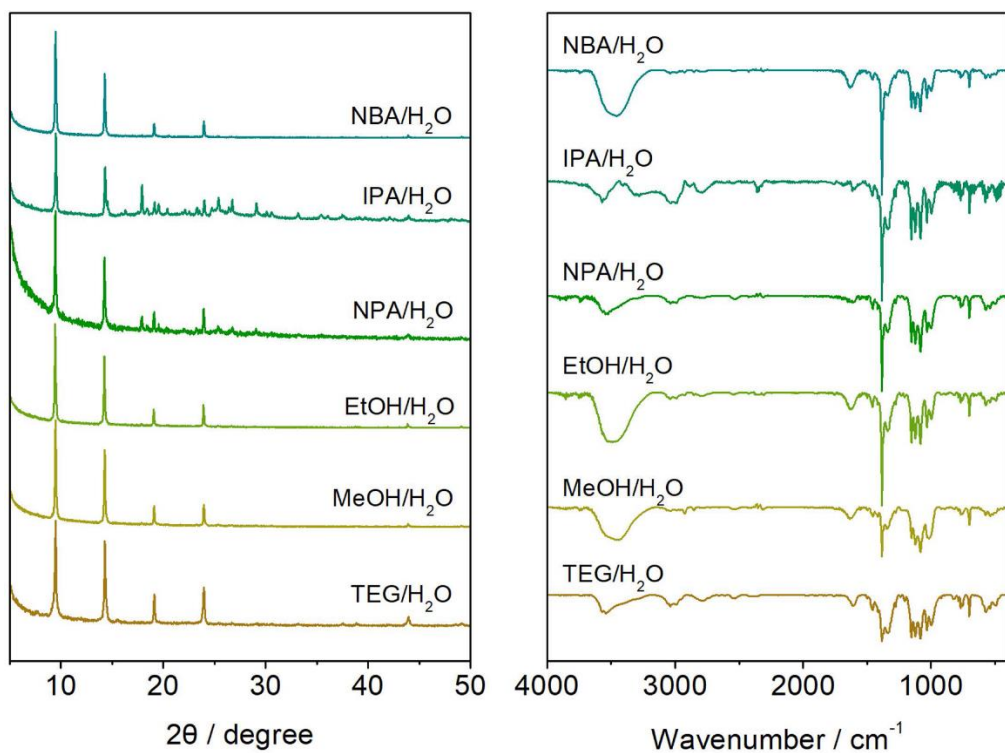


Fig. S25. The PXRD patterns (left) and IR spectra (right) of the $\text{In}(\text{NO}_3)_3/\text{S-pempH}_2$ assemblies obtained in 90 vol% alcohol/ H_2O at 100 °C.

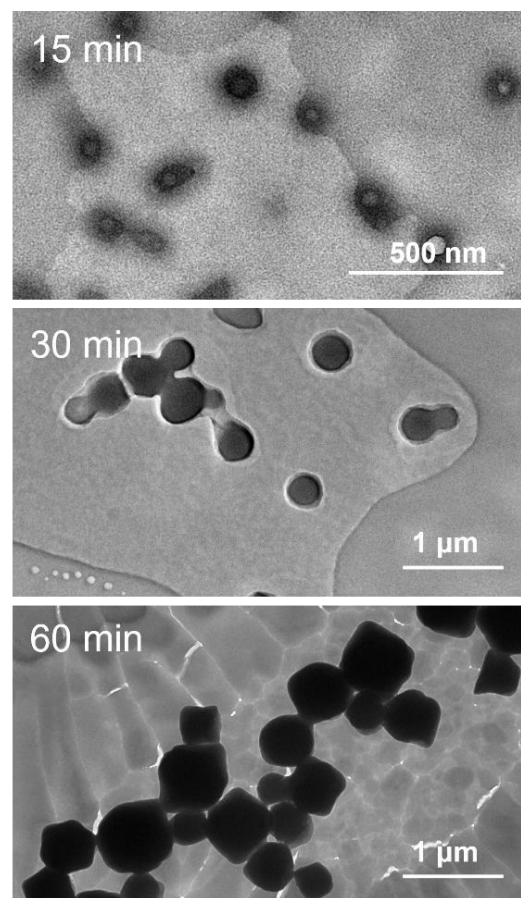


Fig. S26. TEM images of the self-assembled products of $\text{In}(\text{NO}_3)_3/\text{S-pempH}_2$ in 90 vol% IPA/ H_2O at 100 °C before 90 min.

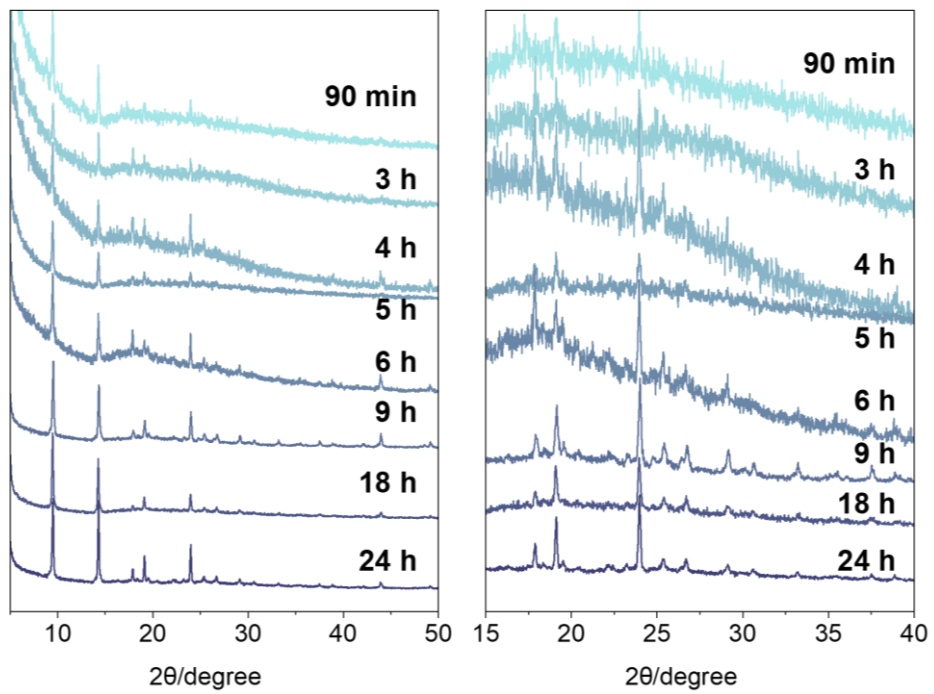


Fig. S27. PXRD patterns of the self-assembled products of $\text{In}(\text{NO}_3)_3/\text{S-pempH}_2$ in 90 vol% IPA/H₂O at 100 °C for different periods of reaction time.

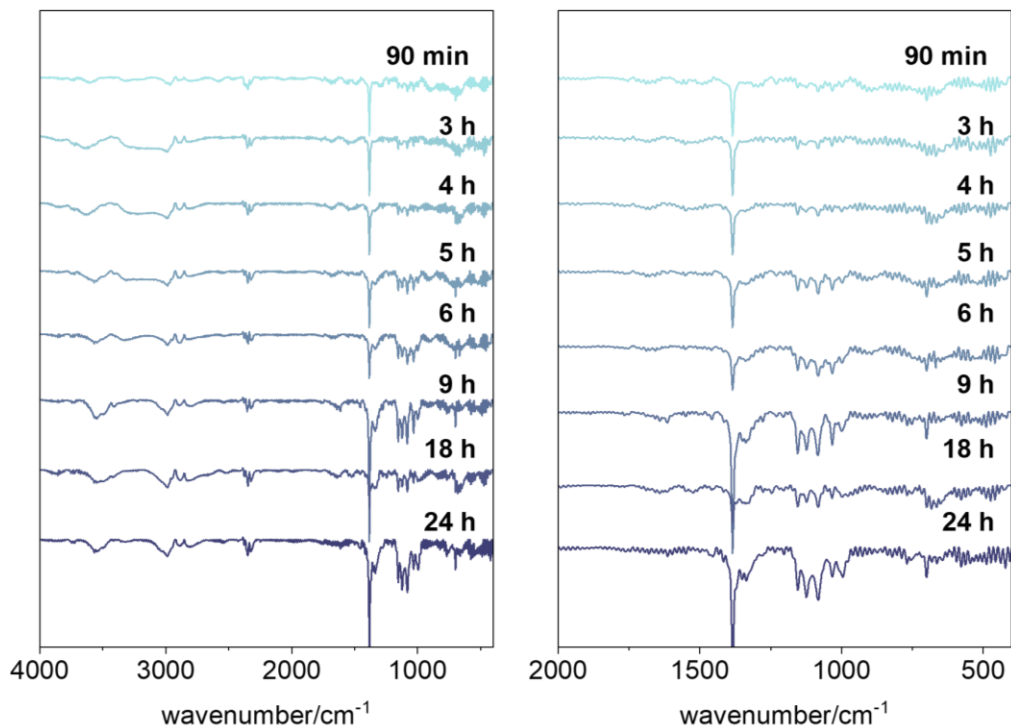


Fig. S28. IR spectra of the self-assembled products of $\text{In}(\text{NO}_3)_3/\text{S-pempH}_2$ in 90 vol% IPA/H₂O at 100 °C for different periods of reaction time.

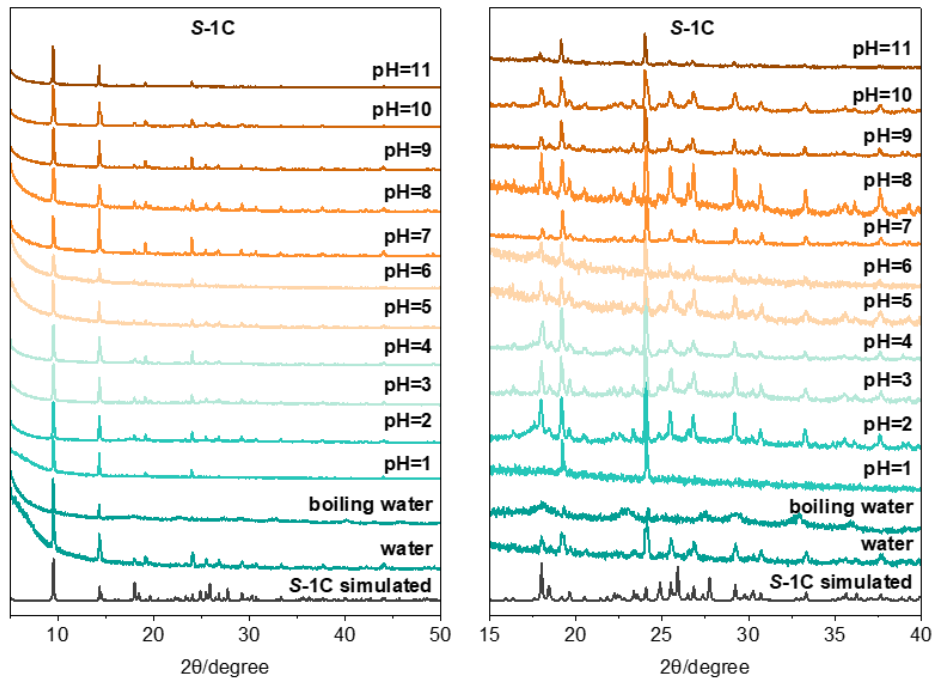


Fig. S29. PXRD patterns of the as-synthesized and post-treated samples of **S-1C** by soaking in water, boiling water and different HCl/NaOH aqueous solutions in the pH range of 1 to 11 for 24 hours.

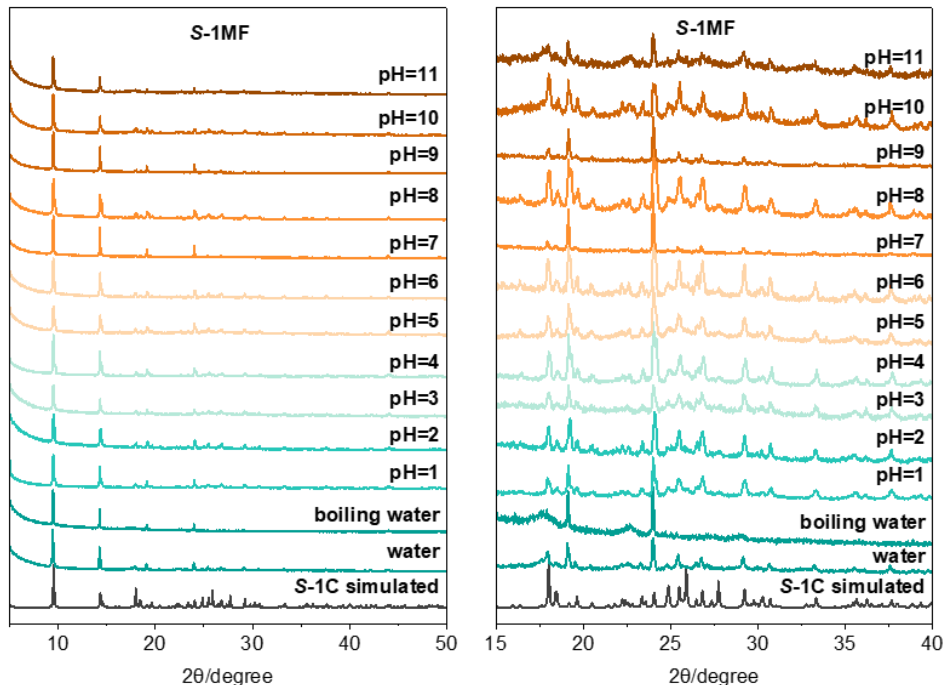


Fig. S30. PXRD patterns of the as-synthesized and post-treated samples of **S-1MF** by soaking in water, boiling water and different HCl/NaOH aqueous solutions in the pH range of 1 to 11 for 24 hours.

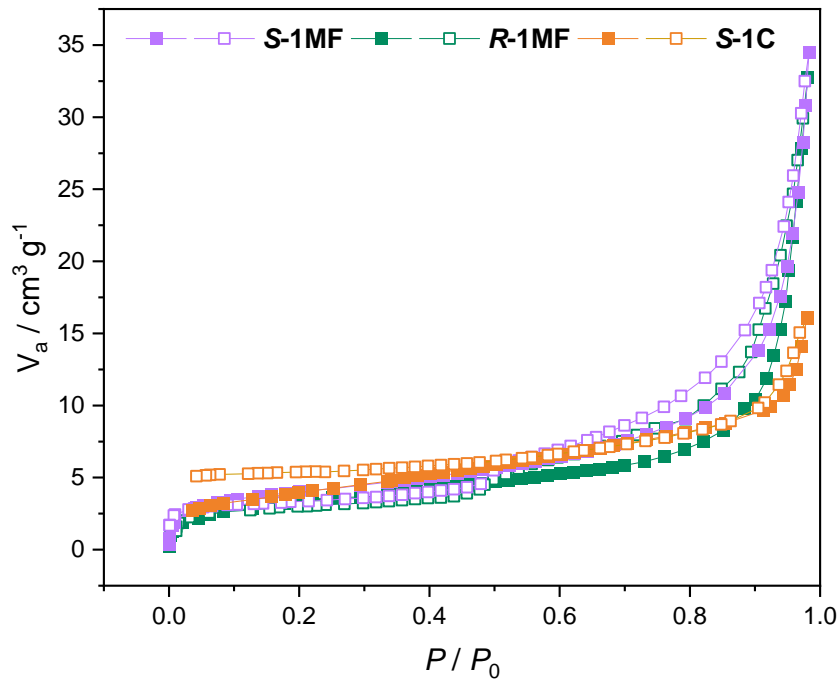


Fig. S31. The N₂ adsorption (filled) and desorption (open) isotherms at 77K for **R-1MF**, **S-1MF**, and **S-1C**.

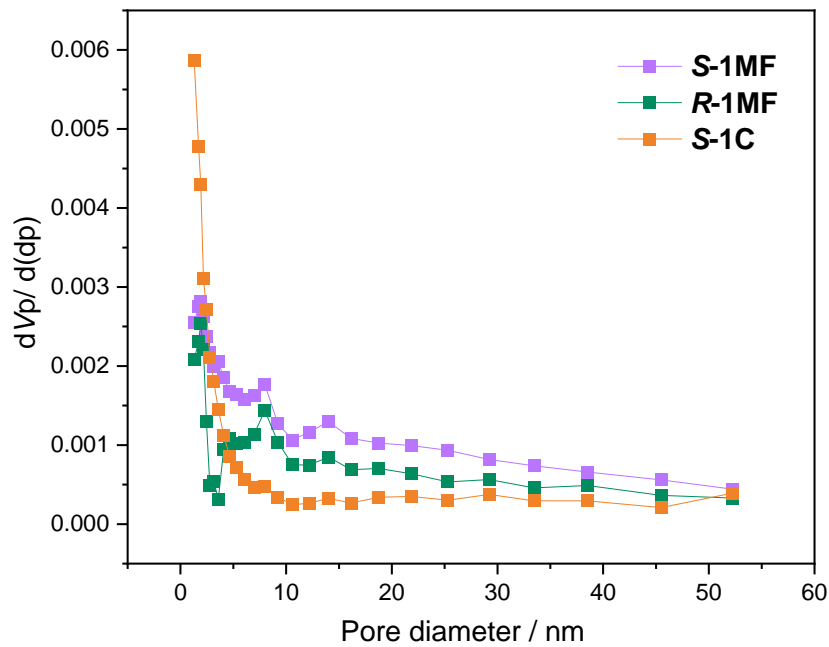


Fig. S32. Barrett-Joyner-Halenda (BJH) pore size distribution of **R-1MF**, **S-1MF**, and **S-1C**.

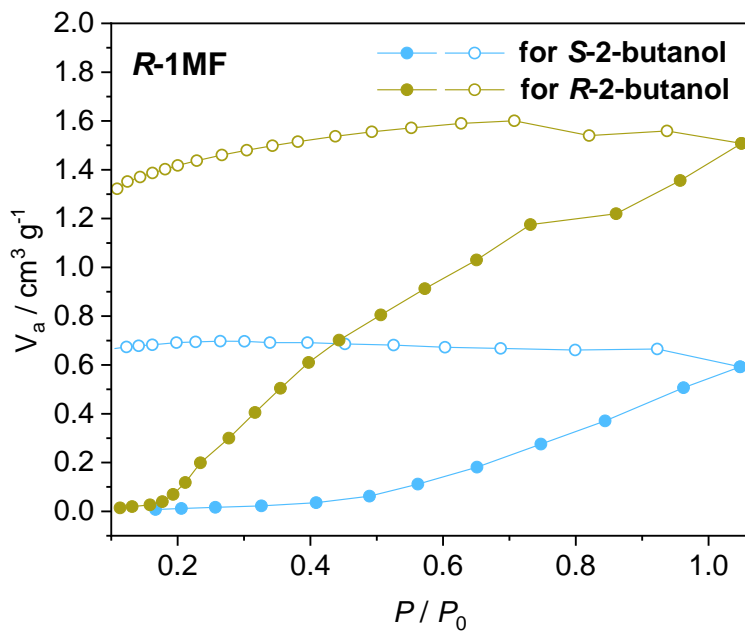


Fig. S33. S- and R-2-Butanol adsorption (filled) and desorption (open) isotherms for activated compounds of **R-1MF** at 298 K.

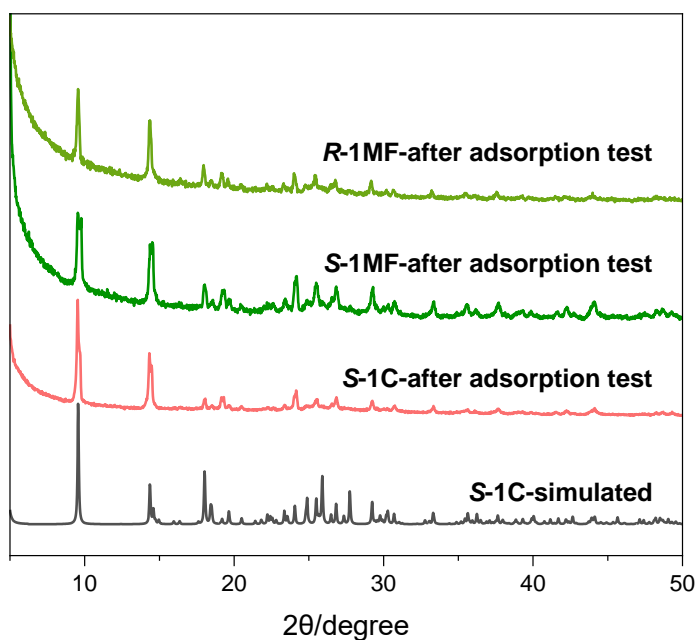


Fig. S34. PXRD patterns of **S-1C**, **S-1MF** and **R-1MF** after adsorption testing. The simulated pattern of **S-1C** is given for comparison.